

SHORT COMMUNICATION

Ground motion selection for seismic slope displacement analysis using a generalized intensity measure distribution method

Wenqi Du^{1†}  | Gang Wang²

¹Institute of Catastrophe Risk Management, Nanyang Technological University, Singapore

²Department of Civil and Environmental Engineering, Hong Kong University of Science and Technology, Hong Kong

Correspondence

Wenqi Du, Institute of Catastrophe Risk Management, Nanyang Technological University, 50 Nanyang Avenue, Singapore 639798
Email: wqdu@ntu.edu.sg

SUMMARY

Selecting ground motions based on the generalized intensity measure distribution (GIMD) approach has many appealing features, but it has not been fully verified in engineering practice. In this paper, several suites of ground motions, which have almost identical distributions of spectral acceleration (SA) ordinates but different distributions of non-SA intensity measures, are selected using the GIMD-based approach for a given earthquake scenario. The selected ground motion suites are used to compute the sliding displacements of various slopes. Comparisons of the resulting displacements demonstrate that selecting ground motions with biased distribution of some intensity measures (ie, Arias intensity) may yield systematic biases (up to 60% for some slope types). Therefore, compared to the ground motions selected based only on the distribution of SA ordinates, the ground motion suite selected by the GIMD-based approach can better represent the various characteristics of earthquake loadings, resulting in generally unbiased estimation in specific engineering applications.

KEYWORDS

engineering application, generalized intensity measure distribution (GIMD), ground motion selection, seismic slope displacement

1 | INTRODUCTION

Nowadays, dynamic time-history analysis is commonly used for assessing the seismic performance of major structures or infrastructures. The input time series are generally selected from previously recorded earthquake ground motions. Because the ground motion variability has a significant impact on the seismic performance of engineering systems,¹ selecting an appropriate input motion suite is then a critical step in time-history analysis.

Recently, many methods and tools have been developed in selecting ground motions for seismic dynamic analysis (eg, previous studies²⁻⁷). Many of the existing methods are conducted to select ground motions that have response spectra matching a specified target spectrum (eg, Wang et al⁷). Recently, several ground-motion selection algorithms are proposed for matching a target response spectrum mean and variance.^{2,4,5} For some applications, generalized intensity measures (IMs) rather than spectral acceleration (SA) ordinates only need to be considered.^{6,8} The generalized intensity measure distribution (GIMD) approach describes the multivariate distribution of multiple IMs for a given earthquake

[†]Email: wqdu@ntu.edu.sg

scenario. As a special case, the generalized conditional IM method develops a conditional lognormal distribution of multiple IMs, generally conditioned on a specific value of a primary IM.⁸

Although the GIMD-based approach is one of the advanced ground motion selection methods, the application of this approach to engineering systems is still limited. This paper then aims at conducting the GIMD-based ground motion selections using several target vector-IM cases under a deterministic scenario, and comparing the performance of the selected ground motion suites for seismic slope displacement analysis. The displacements computed using various ground motion suites are compared to quantitatively demonstrate the advantage of the GIMD-based ground motion selection method over the conventional methods based on SA ordinates only.

2 | GIMD-BASED GROUND MOTION SELECTION ALGORITHM

In this section, the ground motion selection and modification method proposed by Wang⁴ is updated to consider the distribution of generalized IMs.

2.1 | Multivariate distribution of vector-IM

A vector-IM can be assumed to follow a multivariate normal distribution. For each IM, the mean and the standard deviation can be obtained from a ground motion prediction equation (GMPE). To construct the joint distribution of the vector-IM, the correlations between pairs of IMs are key requirements, which have been studied by various researchers (eg, previous studies⁹⁻¹¹). Therefore, for a given scenario, a set of simulated IM vectors $\ln IM^{\text{simu}}$ should follow specified means and covariance as

$$\ln IM^{\text{simu}} = N(\boldsymbol{\mu}_{\ln IM}, \boldsymbol{\Sigma}_{\ln IM}) \quad (1)$$

where $\boldsymbol{\mu}_{\ln IM}$ denotes the logarithmic means of the vector-IM, $\boldsymbol{\Sigma}_{\ln IM}$ represents the covariance matrix of the vector-IM, and N is a notation for multivariate normal distribution. The $\boldsymbol{\mu}_{\ln IM}$ and $\boldsymbol{\Sigma}_{\ln IM}$ in Equation 1 can be determined either unconditionally or conditionally. Specifically, the generalized conditional IM method approach develops the distribution of multiple IMs conditioned on the occurrence of a specific value of a primary IM, commonly represented by SA at a given period. More mathematical details about the derivative process of the conditional approach can be found in Jayaram et al.⁵

2.2 | Realizations of the simulated IM vectors

Following the statistical distribution defined in Equation 1, a suite of N IM vectors ($\ln IM^{\text{simu}_m}$, $m = 1, 2, \dots, N$) can be randomly realized on the basis of the Cholesky decomposition. This procedure needs to be repeated for a certain number of times. Among these suites of realizations, one can identify a suite of simulated IM vector whose statistical distribution best represents the statistical parameters ($\boldsymbol{\mu}_{\ln IM}$, $\boldsymbol{\Sigma}_{\ln IM}$) in Equation 1. The suite is defined as the optimal simulated suite.

2.3 | Selection of recorded ground motions

For each simulated IM vector in the optimal suite, one recorded ground motion can be scaled and selected from a specific ground motion database, based on the closely match to the simulated IM vector. A weighted sum of squared errors ($WSSE$) is used to quantify the mismatch between simulated and recorded IM vectors, which is computed as

$$WSSE = \sum_{i=1}^{N_{im}} w_i [\ln IM_i^{\text{simu}_m} - \ln(SF^\alpha \cdot IM_i^{\text{record}})]^2 \quad (2)$$

where $IM_i^{\text{simu}_m}$ is the i -th ($i = 1, 2, \dots, N_{im}$) IM value of the m -th simulated IM vector, SF denotes the scale factor and α is used to differentiate the effect of SF on various IMs, w_i is the assigned weight to the i -th IM, and IM_i^{record} is the recorded i -th IM value.

For each recorded ground motion, the SF value can be determined by minimizing $WSSE$. Therefore, for a simulated IM vector, the scaled recorded ground motion that yields the minimum $WSSE$ would be selected. The process is repeated for each simulated IM vector in the optimal suite until an ensemble of N scaled records is obtained.

2.4 | Refinement of the selected ground motion suite

In this step, the statistical distribution of the selected recorded ground motion ensemble is compared with the prescribed statistical parameters ($\mu_{\ln IM}$, $\sigma_{\ln IM}$). The global residuals R can be defined as

$$R = \sum_{i=1}^{N_{im}} \left[w_i (\hat{m}_{\ln IM_i} - \mu_{\ln IM_i})^2 + w_i (\hat{s}_{\ln IM_i} - \sigma_{\ln IM_i})^2 \right] \quad (3)$$

where $\hat{m}_{\ln IM_i}$ and $\hat{s}_{\ln IM_i}$ are the sample mean and standard deviation of the i -th logarithmic IM of the selected ground motion ensemble, respectively. Because R denotes the *WSSE* on the logarithmic scale, it represents the sum of the normalized errors for IMs with different units considered. To refine the ground motion suite selected, the procedures listed in Sections 2.2 to 2.4 should be repeated for a certain number of times. This is called a replicate selection procedure. Among these selected ground motion suites, the suite that minimizes the total residuals R is identified as the final ground motion suite.

The proposed algorithm is conceptually similar to some previously introduced algorithms.^{4,8} Our experiences imply that the proposed algorithm can generate a suite of ground motions with proper match to the prescribed statistical distribution of a target vector-IM set, which will be illustrated in Section 3.

3 | APPLICATION OF THE GIMD-BASED GROUND MOTION SELECTION APPROACH

In this section, the GIMD-based ground motion selection method is performed for a deterministic scenario, and several suites of ground motions are selected on the basis of various target vector-IM cases. The database used in this study is a subset of the PEER NGA-West2 database.¹² Some low-quality, unreliable, incomplete, nonfree-field recordings, and nonshallow-crustal earthquakes are removed from the original database, resulting in a number of 15 133 recordings in the final database.

3.1 | Earthquake scenario and various target vector-IM cases for ground motion selection

An earthquake scenario with moment magnitude (M_w) 7 occurred on a strike-slip fault is considered. The assumed rupture distance (R_{rup}) is 20 km, and the averaged shear wave velocity in the upper 30 m (V_{s30}) of this site is 400 m/s. The other parameters assigned are dip angle 90°, rake angle 180°, depth to the top of the rupture plane Z_{tor} as 0 km, and the depth to the 2.5 km/s shear wave velocity horizon $Z_{2.5}$ as 2 km. They are input parameters for predicting the distribution of IMs by GMPes.

A series of IMs is then considered as “target” to select ground motions under this earthquake scenario. The full target vector-IM includes SA ordinates at 22 periods, Arias intensity I_a , and significant duration $D_{S_{5-75}}$. The GMPes in the literature¹³⁻¹⁵ are used for predicting the distributions (means and standard deviations) of these IMs, respectively. The empirical correlation equations proposed by Baker and Jayaram⁹ and Bradley^{10,11} are adopted to estimate the SA-SA, SA- $D_{S_{5-75}}$, and SA- I_a correlations, respectively. The correlation coefficient between I_a and $D_{S_{5-75}}$ is assigned as -0.19 .¹⁰ They are used to construct the covariance matrix among these IMs. It should be noted that only the unconditional target distribution of the IMs is considered herein, because this study focuses on investigating the dynamic performance of various kinds of slopes. We did not specify a bounding criterion for magnitude and rupture distance in the selection process; alternatively, the scale factors are limited within the range of 0.25 to 4 to avoid excessive scaling of ground motions. The number of replicate selections is set as 5. In each suite, the number of the selected ground motions is set as 60. The corresponding weights (w_i in Equations 2 and 3) for SA at $T < 1$ s and non-SA IMs are assigned as 2, and the weights for SA ordinates at $T > 1$ s are 1 accordingly.

Besides the standard target vector-IM case, several target cases are also considered for comparison purposes. The specific target means of the 5 vector-IM cases are listed in Table 1. Case A represents the unbiased consideration of the target vector-IM. Cases B to E represent the target vector-IMs that the mean target of one non-SA IM is intentionally perturbed. Using the target cases B to E, the selected ground motions would anticipatively display a biased distribution of the specific IM (ie, I_a or $D_{S_{5-75}}$), but they generally keep unbiased distributions of the SA ordinates. Thus, the selected ground motions based on cases B and C (D and E) can be used to scrutinize the corresponding effect of I_a ($D_{S_{5-75}}$) on engineering applications.

TABLE 1 Various means of the target vector-IM cases for ground motion selection

Case	A	B	C	D	E
SA(T)	μ	μ	μ	μ	μ
Ia	μ	$\mu + 0.5\sigma$	$\mu - 0.5\sigma$	μ	μ
Ds ₅₋₇₅	μ	μ	μ	$\mu + 0.5\sigma$	$\mu - 0.5\sigma$

μ and σ denote the predicted mean and standard deviation for each IM obtained from GMPES.

Table 2 shows the statistical distributions of the causal parameters and scaling factors for the ground motion suites of A to E. The average scale factors assigned for the 5 suites are around 1.5 to 2. As mentioned previously, no bounding criterion for these causal parameters was considered during the selection process. The mean M_w and V_{s30} values of the selected suites are generally in good agreement with the prescribed values; the mean R_{rup} values of the selected suites are larger than 20 km, which is not surprising because of the limited number of the short distance records ($R_{rup} < 20$ km) in the database. In general, it can be seen that the distributions of these parameters for various cases are within a reasonable range.

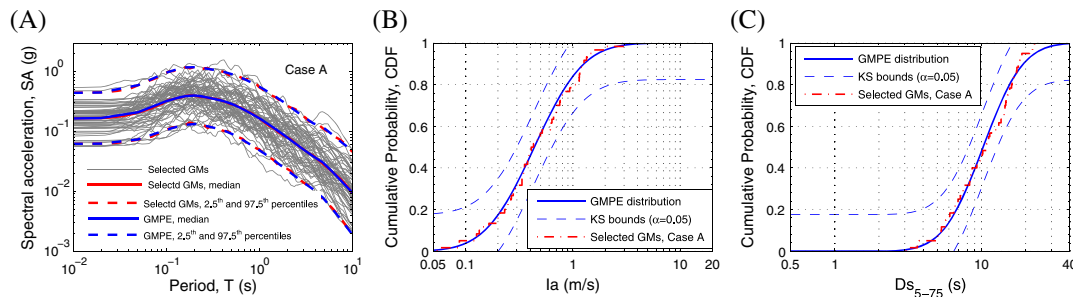
3.2 | Ground motion characteristics selected based on the defined vector-IM cases

Figure 1A shows the response spectra of the selected ground motions using the vector-IM case A. The median, 2.5th and 97.5th percentiles of the selected SA ordinates are also compared to the target distribution. It can be seen that the selected ground motion suite can properly represent the target distribution of SA ordinates over a wide period range. Figure 1B,C presents the empirical cumulative distribution functions (CDFs) of Ia and Ds₅₋₇₅ of the selected ground motions for case A, respectively. The statistical distributions as well as the KS bounds at 5% significance level are also plotted in these plots, from which it can be seen that the selected ground motion suite shows appropriate distributions for these IMs.

Figure 2A displays the median, 2.5th and 97.5th percentiles of the selected SA ordinates using the vector-IM cases B and C. The statistical target distribution obtained by the GMPE¹³ is also plotted in this plot. Figure 2B,C shows the

TABLE 2 Statistical distributions of the causal parameters and scale factors for the selected ground motion suites A-E

Scenario considered	$M_w = 7$		$R_{rup} = 20$ km		$V_{s30} = 400$ m/s		Scale factor (0.25-4)		
	Mean	St.d.	Mean	St.d.	Mean	St.d.	Mean	St.d.	
Selected GM suites	A	6.91	0.49	51.0	39.5	426.7	274.8	1.84	1.24
	B	7.04	0.39	59.5	44.0	429.3	183.5	1.99	1.07
	C	6.80	0.55	53.8	46.1	386.9	181.2	1.68	1.05
	D	6.94	0.56	61.9	47.4	394.3	219.5	1.99	1.20
	E	7.00	0.42	46.3	39.3	443.4	218.1	1.59	1.06

**FIGURE 1** A, Spectral distributions of the selected 60 ground motions for IM-vector case A. B, C, Cumulative distributions of Ia and Ds₅₋₇₅ for the IM-vector case A, respectively [Colour figure can be viewed at wileyonlinelibrary.com]

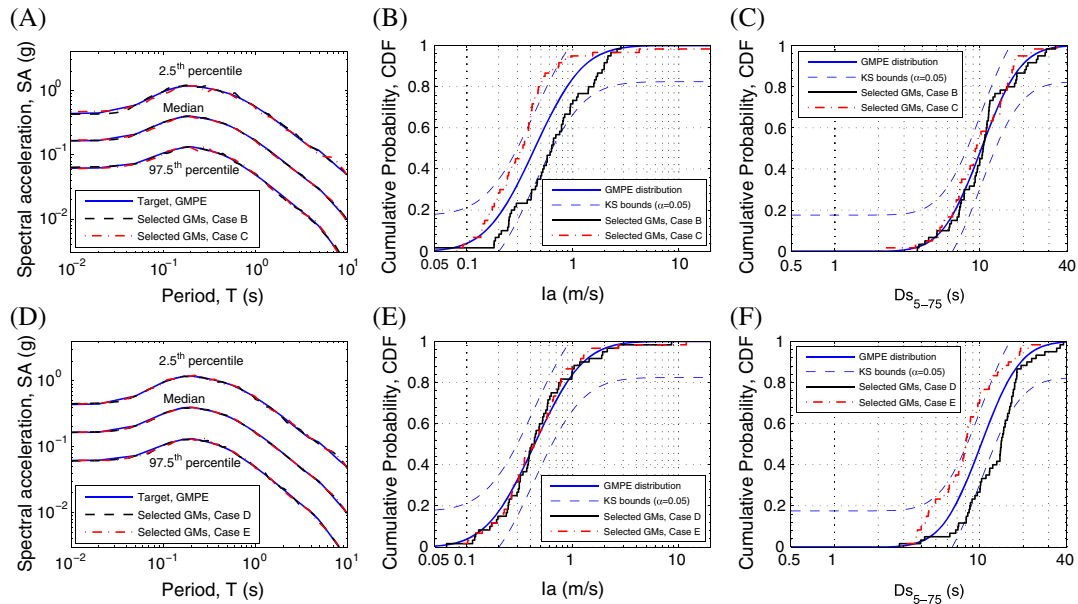


FIGURE 2 A, Spectral distributions of the selected ground motions for IM-vector cases B and C. B, C, Cumulative distributions of I_a and $D_{S_{5-75}}$ for cases B and C, respectively. D, Spectral distributions of the selected ground motions for IM-vector cases D and E. E, F, Cumulative distributions of I_a and $D_{S_{5-75}}$ for cases D and E, respectively [Colour figure can be viewed at wileyonlinelibrary.com]

cumulative distributions of the non-SA IMs of the selected ground motions using the 2 vector-IM cases, respectively. As expected, the matches between the empirical and the GMPE distributions for SA and $D_{S_{5-75}}$ are generally good; the cumulative distributions of I_a for cases B and C are systematically larger and smaller than the statistical distribution, respectively. Similarly, Figure 2D illustrates appropriate representations for SA ordinates of the selected ground motion suites D and E. Figure 2E,F shows the comparisons of the empirical CDFs of the non-SA IMs with the corresponding statistical distributions, respectively. The ground motion suites D and E have generally unbiased representations for the distributions of SA ordinates and I_a , while they have distinctively different representations for the distribution of $D_{S_{5-75}}$. As seen from Figures 1 and 2, the selected ground motion suites for cases A to E can generally meet the “target” requirements specified in Table 1.

4 | SEISMIC SLOPE DISPLACEMENT ANALYSIS USING THE SELECTED GROUND MOTION SUITES

Evaluation of the coseismic sliding displacement is important in assessing the seismic stability of slopes. Newmark¹⁶ firstly proposed a rigid sliding block model, which assumed that sliding is initialized when the shaking exceeds yield acceleration (K_y), and the rigid-block slides plastically along a predefined shear surface. Since then, many predictive equations have been developed using the Newmark rigid-block model (eg, Jibson¹⁷). The Newmark model is only applicable to natural, shallow slopes.

Many studies have been conducted to evaluate the seismic performance of deep/flexible sliding masses. One of the widely used methods is the nonlinear fully coupled stick-slip sliding block analysis.¹⁸ This method models the dynamic response of a sliding mass and computes the sliding displacement simultaneously. It provides a more realistic representation of the dynamic performance of flexible slopes. In this study, the seismic sliding displacements of various slopes are calculated using the equivalent-linear coupled stick-slip sliding mass model.¹⁹ The stiffness and dynamic strength of a sliding mass are characterized by its initial fundamental period (T_s) and K_y , respectively. T_s and K_y can be commonly expressed as a function of slope properties. The detailed procedures of this model and the soil parameters assigned can be found in Wang.¹⁹

The sliding displacements D based on the combination of T_s and K_y are computed using the 5 selected ground motion suites. The values of T_s and K_y are assigned ranging from 0.01 to 2 seconds, and from 0.01 to 0.2 g, respectively. Figure 3 demonstrates the empirical CDFs of the calculated displacements for 2 slope (T_s , K_y) cases. Since displacements smaller

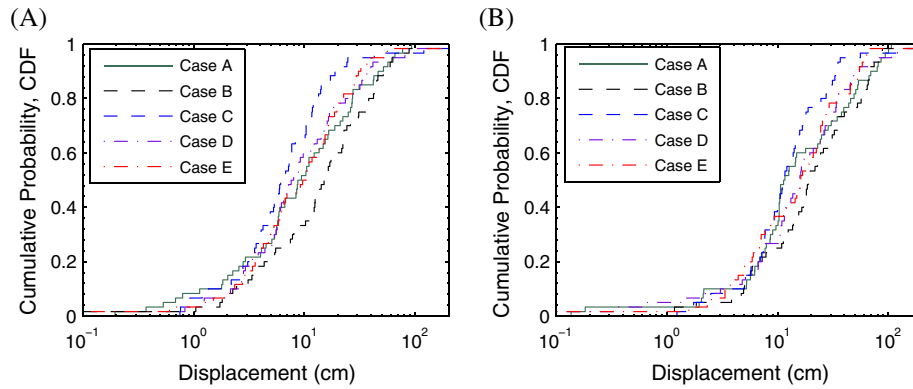


FIGURE 3 Empirical CDFs of the calculated displacements for slope cases A, $T_s = 0.1$ s, $K_y = 0.05$ g; B, $T_s = 0.5$ s, $K_y = 0.05$ g [Colour figure can be viewed at [wileyonlinelibrary.com](#)]

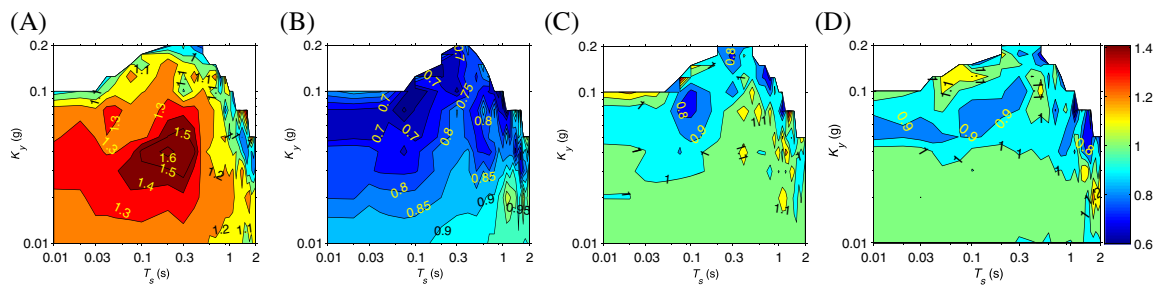


FIGURE 4 The ratios of the computed mean displacements \bar{D} using selected ground motions A, suite B, B, suite C, C, suite D, and D, suite E to those of the ground motion suite A, respectively [Colour figure can be viewed at [wileyonlinelibrary.com](#)]

than 1 cm are commonly recognized as negligible in engineering applications, only D larger than 1 cm are used to compute the mean displacement \bar{D} for each slope (T_s , K_y) case. Figure 4A to D displays the ratios of the mean displacements \bar{D} for ground motion suites B, C, D, and E to those of the benchmark suite A, respectively. As shown in Figure 4A,B, the computed \bar{D} using ground motion suites with biased distributions of Ia result in systematic biases for most types of slopes. Although the 3 suites (A, B, C) have similar distributions of SA ordinates, the computed mean displacements generally increase with the increase of Ia amplitudes. The results reveal the strong correlation between Ia and the slope displacements especially for rigid and moderate slopes, which is in accordance with previous studies (eg, Jibson¹⁷ and Du and Wang²⁰). Therefore, Ia must be considered in the target vector-IM to select representative ground motions for slope displacement analysis. On the other hand, compared to the results of suite A, the computed mean displacements using ground motion suites with biased distribution of D_{5-75} (suites D, E) would not cause noticeable differences, as illustrated in Figure 4C,D.

5 | CONCLUSIONS

Selecting ground motions based on the GIMD is one of the latest methods in ground motion selection. The application of the GIMD-based approach to seismic slope displacement analysis was demonstrated in this study. For a given earthquake scenario, 5 suites of ground motions were selected using different cases of target vector-IM. The target vector-IM consisted of SA ordinates, Ia, and D_{5-75} . All the selected ground motion suites have unbiased distributions of SA ordinates, associated with the various constraints of distributions of the non-SA IMs. The selected ground motion suites were used to compute the sliding displacements of a variety of slopes. It was observed that the ground motions selected with biased distribution of Ia would result in systematic biases up to 60% for the computed slope displacements, while the selected ground motions with biased distribution of D_{5-75} would not bring in notable biases. This study quantitatively highlights the importance of considering some non-SA IMs, in addition to the SA ordinates during the ground motion selection process.

This study also provides a method for examining the effect of a given IM on the seismic performance of specific engineering systems. For instance, the influence of ground motion duration on structural responses is still under debate. The methodology presented in this paper can reasonably decouple the effect of duration from other ground motion characteristics, and it could provide useful insights on such research topics.

ACKNOWLEDGEMENTS

The work described in this paper was supported by HK Research Grants Council through General Research Fund grant no. 16213615. The author thanks 2 anonymous reviewers for their helpful comments to improve this manuscript.

ORCID

Wenqi Du  <http://orcid.org/0000-0002-4392-6255>

REFERENCES

1. Rathje EM, Kottke AR, Trent WL. Influence of input motion and site property variabilities on seismic site response analysis. *J Geotech Geoenviron Eng*. 2010;136(4):607-619. [https://doi.org/10.1061/\(ASCE\)GT.1943-5606.0000255](https://doi.org/10.1061/(ASCE)GT.1943-5606.0000255)
2. Baker JW. Conditional mean spectrum: tool for ground-motion selection. *J Struct Eng*. 2010;137(3):322-331.
3. Bradley BA. A generalized conditional intensity measure approach and holistic ground-motion selection. *Earthq Eng Struct Dyn*. 2010;39(12):1321-1342.
4. Wang G. A ground motion selection and modification method capturing response spectrum characteristics and variability of scenario earthquakes. *Soil Dyn Earthq Eng*. 2011;31(4):611-625. <https://doi.org/10.1016/j.soildyn.2010.11.007>
5. Jayaram N, Lin T, Baker JW. A computationally efficient ground-motion selection algorithm for matching a target response spectrum mean and variance. *Earthq Spectra*. 2011;27(3):797-815. <https://doi.org/10.1193/1.3608002>
6. Bradley BA. A ground motion selection algorithm based on the generalized conditional intensity measure approach. *Soil Dyn Earthq Eng*. 2012;40:48-61. <https://doi.org/10.1016/j.soildyn.2012.04.007>
7. Wang G, Youngs R, Power M, Li Z. Design ground motion library (DGML): an interactive tool for selecting earthquake ground motions. *Earthq Spectra*. 2015;31(2):617-635. <https://doi.org/10.1193/090612EQS283M>
8. Tarbali K, Bradley BA. Ground motion selection for scenario ruptures using the generalised conditional intensity measure (GCIM) method. *Earthq Eng Struct Dyn*. 2015;44(10):1601-1621. <https://doi.org/10.1002/eqe.2546>
9. Baker JW, Jayaram N. Correlation of spectral acceleration values from NGA ground motion models. *Earthq Spectra*. 2008;24(1):299-317. <https://doi.org/10.1193/1.2857544>
10. Bradley BA. Correlation of significant duration with amplitude and cumulative intensity measures and its use in ground motion selection. *J Earthq Eng*. 2011;15(6):809-832. <https://doi.org/10.1080/13632469.2011.557140>
11. Bradley BA. Correlation of arias intensity with amplitude, duration and cumulative intensity measures. *Soil Dyn Earthq Eng*. 2015;78:89-98. <https://doi.org/10.1016/j.soildyn.2015.07.009>
12. Ancheta TD, Darragh RB, Stewart JP, et al. NGA-West2 database. *Earthq Spectra*. 2014;30(3):989-1005. <https://doi.org/10.1193/070913EQS197M>
13. Campbell KW, Bozorgnia Y. NGA ground motion model for the geometric mean horizontal component of PGA, PGV, PGD and 5% damped linear elastic response spectra for periods ranging from 0.1 to 10 s. *Earthq Spectra*. 2008;24(1):139-171. <https://doi.org/10.1193/1.2857546>
14. Campbell KW, Bozorgnia Y. A comparison of ground motion prediction equations for Arias intensity and cumulative absolute velocity developed using a consistent database and functional form. *Earthq Spectra*. 2012;28(3):931-941. <https://doi.org/10.1193/1.4000067>
15. Du W, Wang G. Prediction equations for ground motion significant durations using the NGA-West2 database. *Bull Seismol Soc Am*. 2017;107(1):319-333. <https://doi.org/10.1785/0120150352>
16. Newmark NM. Effects of earthquakes on dams and embankments. *Géotechnique*. 1965;15(2):139-160. <https://doi.org/10.1680/geot.1965.15.2.139>
17. Jibson RW. Regression models for estimating coseismic landslide displacement. *Engineering Geology*. 2007;91(2):209-218. <https://doi.org/10.1016/j.enggeo.2007.01.013>
18. Rathje EM, Bray JD. Nonlinear coupled seismic sliding analysis of earth structures. *J Geotech Geoenviron Eng*. 2000;126(11):1002-1014. [https://doi.org/10.1061/\(ASCE\)1090-0241\(2000\)126:11\(1002\)](https://doi.org/10.1061/(ASCE)1090-0241(2000)126:11(1002))
19. Wang G. Efficiency of scalar and vector intensity measures for seismic slope displacements. *Front Struct Civ Eng*. 2012;6(1):44-52.

20. Du W, Wang G. Fully probabilistic seismic displacement analysis of spatially distributed slopes using spatially correlated vector intensity measures. *Earthq Eng Struct Dyn*. 2014;43(5):661-679. <https://doi.org/10.1002/eqe.2365>

How to cite this article: Du W, Wang G. Ground motion selection for seismic slope displacement analysis using a generalized intensity measure distribution method. *Earthquake Engng Struct Dyn*. 2018;47:1352–1359. <https://doi.org/10.1002/eqe.2998>